Both brown adipose tissue and skeletal muscle thermogenesis processes are activated during mild to severe cold adaptation in mice

Received for publication, April 13, 2017, and in revised form, July 24, 2017 Published, Papers in Press, August 9, 2017, DOI 10.1074/jbc.M117.790451

Naresh C. Bal[‡§¶1], Sushant Singh[§¶], Felipe C. G. Reis[¶], Santosh K. Maurya[§¶], Sunil Pani[‡], Leslie A. Rowland[§], and Muthu Periasamy[§¶2]

From the [‡]School of Biotechnology, KIIT University, Bhubaneswar, Odisha 751024, India, the [§]Department of Physiology and Cell Biology, College of Medicine, Ohio State University, Columbus, Ohio 43210, and the [¶]Sanford Burnham Prebys Medical Discovery Institute at Lake Nona, Orlando, Florida 32827

Edited by John M. Denu

Thermogenesis is an important homeostatic mechanism essential for survival and normal physiological functions in mammals. Both brown adipose tissue (BAT) (*i.e.* uncoupling protein 1 (UCP1)-based) and skeletal muscle (*i.e.* sarcolipin (SLN)-based) thermogenesis processes play important roles in temperature homeostasis, but their relative contributions differ from small to large mammals. In this study, we investigated the functional interplay between skeletal muscle- and BAT-based thermogenesis under mild *versus* severe cold adaptation by employing $UCP1^{-/-}$ and $SLN^{-/-}$ mice. Interestingly, adaptation of $SLN^{-/-}$ mice to mild cold conditions (16 °C) significantly increased UCP1 expression, suggesting increased reliance on BAT-based thermogenesis. This was also evident from structural alterations in BAT morphology, including mitochondrial architecture, increased expression of electron transport chain proteins, and depletion of fat droplets. Similarly, $UCP1^{-/-}$ mice adapted to mild cold up-regulated muscle-based thermogenesis, indicated by increases in muscle succinate dehydrogenase activity, SLN expression, mitochondrial content, and neovascularization, compared with WT mice. These results further confirm that SLN-based thermogenesis is a key player in muscle nonshivering thermogenesis (NST) and can compensate for loss of BAT activity. We also present evidence that the increased reliance on BAT-based NST depends on increased autonomic input, as indicated by abundant levels of tyrosine hydroxylase and neuropeptide Y. Our findings demonstrate that both BAT and muscle-based NST are equally recruited during mild and severe cold adaptation and that loss of heat production from one thermogenic pathway leads to increased recruitment of the other, indicating a functional interplay between these two thermogenic processes.

This work was supported in part by National Institutes of Health Grants R01-HL-088555 and R01 DK098240-01 and American Diabetes Association Basic Science Research Award (7-13-BS-131) (to M. P.). The research reported in this work was supported in part by NIDDK, National Institutes of Health under Award DK102772 and a Ramalingaswamy re-entry fellowship from the Department of Biotechnology, India (to N. C. B.). The authors declare that they have no conflicts of interest with the contents of this article. The content is solely the responsibility of the authors and does not necessarily represent the official views of the National Institutes of Health.

[1] To whom correspondence may be addressed. E-mail: naresh.bal@kiitbiotech.ac.in.

[2] To whom correspondence may be addressed. E-mail: mperiasamy@sbpdiscovery.org.

Thermogenesis is an important homeostatic mechanism essential for survival and normal physiological functions in mammals. In mice, BAT is a highly specialized organ and serves as a major site of nonshivering thermogenesis (NST)[3] at both neonatal and adult stages (1, 2). Studies have shown that uncoupling protein 1 (UCP1)-mediated dissipation of the proton gradient in mitochondria is the basis of heat generation in BAT (3–5). Intriguingly, UCP1 knockout ($UCP1^{-/-}$) mice were found to be sensitive to acute cold exposure but could be gradually adapted to severe cold (4 °C), suggesting the existence of other sites for NST. In addition to BAT, skeletal muscle has been suggested to be an important site of NST in mammals (6, 7). Recent work from our laboratory has demonstrated that sarcolipin (SLN), a regulator of the sarco/endoplasmic reticulum Ca^{2+}-ATPase (SERCA) pump, plays an important role in muscle-based NST (8–12). We showed that loss of SLN can severely compromise muscle-based heat production and whole-body temperature maintenance (9, 13). Therefore, we explored whether muscle- and BAT-based thermogenesis work together during cold adaptation. We recently reported that skeletal muscle—based thermogenesis can compensate for loss of BAT thermogenesis in $UCP1^{-/-}$ mice (13).

Despite recent advances in our understanding of the roles played by BAT and muscle in temperature homeostasis, it is unclear whether a functional coordination exists between the two systems. Although it is speculated that a direct cross-talk between BAT and skeletal muscle might exist (14–17), the mechanism is presently not known. There are many unanswered questions, such as whether these two systems are recruited by a common pathway, whether the recruitment of BAT and skeletal muscle relies on signals from the hypothalamus and central nervous system, and whether there is a hierarchy of recruitment. Furthermore, it is also unknown to what extent these two systems can compensate for each other during different degrees of cold adaptations. To address some of these questions, we took advantage of genetically altered mouse models ($UCP1^{-/-}$ and $SLN^{-/-}$ mice) and explored the functional

[3] The abbreviations used are: NST, non-shivering thermogenesis; BAT, brown adipose tissue; SLN, sarcolipin; SERCA, sarco/endoplasmic reticulum Ca^{2+}-ATPase; Tc, core body temperature; TH, tyrosine hydroxylase; NPY, Neuropeptide Y; FFPE, formalin-fixed, paraffin-embedded; ANOVA, analysis of variance; CD, cluster of differentiation; SDH, succinate dehydrogenase.

interplay between muscle and BAT. We especially investigated how these two thermogenic sites are able to compensate for the loss of one another during mild (16 °C) and severe (4 °C) cold adaptation. We further tested the hypothesis that muscle-based NST can be hyper-recruited in the absence of BAT function by challenging UCP1$^{-/-}$ mice to mild cold, a low level of cold stimulus that does not evoke shivering response in skeletal muscle (18).

The findings of this study reveal that even a mild cold (16 °C) challenge was sufficient to evoke a significant remodeling of both BAT and skeletal muscle, suggesting that both systems are recruited during mild cold adaptation. The most interesting finding was that loss of SLN in muscle led to a robust up-regulation of UCP1 expression, along with structural remodeling of BAT even under mild cold, corroborating our central idea that muscle NST is an important component of cold adaptation. The results from this study also suggest that there is a functional interplay between BAT and muscle that can be recruited to compensate for the loss of one another, although the exact mechanism remains less well-understood.

Results

UCP1$^{-/-}$ mice require more energy during cold adaptation

Several earlier studies have shown that, cold adaptation comes at a significant energy cost. Therefore, we used indirect calorimetry to determine whole-body oxygen consumption (VO_2), an index of energy expenditure of the animal. As shown in Fig. 1*A*, regardless of genotype, cold exposure increased VO_2. At thermoneutrality, SLN$^{-/-}$ and UCP1$^{-/-}$ mice consumed less oxygen compared with the WT, suggesting that they contribute to the basal metabolic rate. Interestingly, when housed at 4 °C, VO_2 of UCP1$^{-/-}$ mice was significantly higher compared with WT mice, indicating that increased reliance on muscle-based thermogenesis is energetically more costly. On the other hand, SLN$^{-/-}$ mice consumed less oxygen compared with UCP1$^{-/-}$ littermates, which may indicate that BAT-based NST is energetically more efficient. Intriguingly, during cold challenge, SLN$^{-/-}$ mice showed a high degree of fluctuation in core body temperature (Tc) compared with the WT and were unable to maintain a constant Tc, especially during the first few days of cold exposure (Fig. 1*B*). In contrast, UCP1$^{-/-}$ mice were able to maintain a constant Tc during the whole period of cold challenge, like the WT littermates. In comparison with the WT, both SLN$^{-/-}$ and UCP1$^{-/-}$ mice showed a decrease in body weight (Fig. 1*C*). We found that this decrease in body weight is primarily due to loss of fat deposits without changes in muscle mass. During mild cold, UCP1$^{-/-}$ mice consumed more food than WT mice (Fig. 1*D*). Under extreme cold, both UCP1$^{-/-}$ and SLN$^{-/-}$ mice consumed a similar amount of food, much more than the WT. All of these data, taken together, suggest that an optimal combination of BAT and skeletal muscle—based NST is important and that loss of either requires extra energy investment for Tc maintenance.

Loss of SLN up-regulates UCP1-based thermogenesis even under mild cold

A major objective of this study was to determine whether there is a hierarchy in the recruitment of BAT *versus* skeletal muscle–based thermogenesis and, when SLN is absent, whether BAT-based thermogenesis is hyper-recruited during cold adaptation, especially under mild cold. For cold adaptation studies, mice were reared and maintained at thermoneutrality (29 °C ± 1.0 °C), a housing temperature that does not activate cold-induced thermogenesis (19). To study the impact of mild and severe cold, the housing temperature was decreased to 16 °C ± 1.0 °C (termed mild cold) for 2 weeks and further decreased to 4 °C ± 1.0 °C (termed severe cold) for 2 additional weeks. SLN$^{-/-}$ mice showed a similar level of physical activity at mild cold compared with WT littermates (Fig. 1*E*), and we did not observe any shivering response during housing at 16 °C. We show here that even mild cold adaptation has a significant effect on fat content in BAT of WT and SLN$^{-/-}$ mice. There is a greater loss of fat droplets in SLN$^{-/-}$ mice compared with WT littermates under mild cold, which is further pronounced after extreme cold adaptation (Fig. 2*A*). UCP1 staining was similar between WT and SLN$^{-/-}$ mice at thermoneutrality, but, upon cold exposure, UCP1 expression is induced in both SLN$^{-/-}$ and WT mice. Interestingly, the UCP1 expression level was substantially up-regulated in SLN$^{-/-}$ mice in comparison with WT mice, as shown by immunostaining and Western blot analysis (Fig. 2, *B*—*E*). As the mitochondrial inner membrane is the basis of BAT-based NST, we further examined changes in mitochondrial ultrastructure and the expression of electron transport chain proteins under mild and severe cold. We show that cold adaptation led to up-regulation of complex 1 and 4 in BAT from SLN$^{-/-}$ mice compared with the WT. Moreover, expression of mitochondrial transcription factor A, a regulator of mitochondrial DNA replication and repair, was increased in SLN$^{-/-}$ mice upon cold adaptation. Electron microscopic analyses of the BAT ultrastructure show that, at thermoneutrality, mitochondria contains a less dense crista structure in all three genotypes. On the other hand, even mild cold adaptation induced significant changes in mitochondrial architecture, with a greater density of cristae, in SLN$^{-/-}$ mice compared with WT littermates (Fig. 3). Further exposure to severe cold (4 °C) increased mitochondrial crista density both in WT and SLN$^{-/-}$ mice, but it was more apparent in SLN$^{-/-}$ littermates. The mitochondrial architecture in UCP1$^{-/-}$ mice was, however, unaffected by cold exposure, indicating loss of BAT function.

Muscle-based thermogenesis is hyper-recruited in UCP1$^{-/-}$ mice under mild cold stress

We found that loss of SLN led to an up-regulation of UCP1 even under mild cold challenge; therefore, we next investigated whether loss of UCP1 function leads to enhanced recruitment of skeletal muscle-based thermogenesis. To better define the recruitment of muscle thermogenesis, we studied changes in metabolic activity and mitochondrial structure by performing SDH staining (an index of oxidative metabolism) and electron microscopy of skeletal muscle tissues (Fig. 4). At thermoneutrality, the SDH staining pattern of quadriceps muscle from all three genotypes did not show a marked difference, whereas adaptation to mild cold stress increased SDH activity in quadriceps muscle of UCP1$^{-/-}$ and WT mice but not in SLN$^{-/-}$ mouse muscle (Fig. 4*A*). At 4.0 °C, quadriceps from UCP1$^{-/-}$

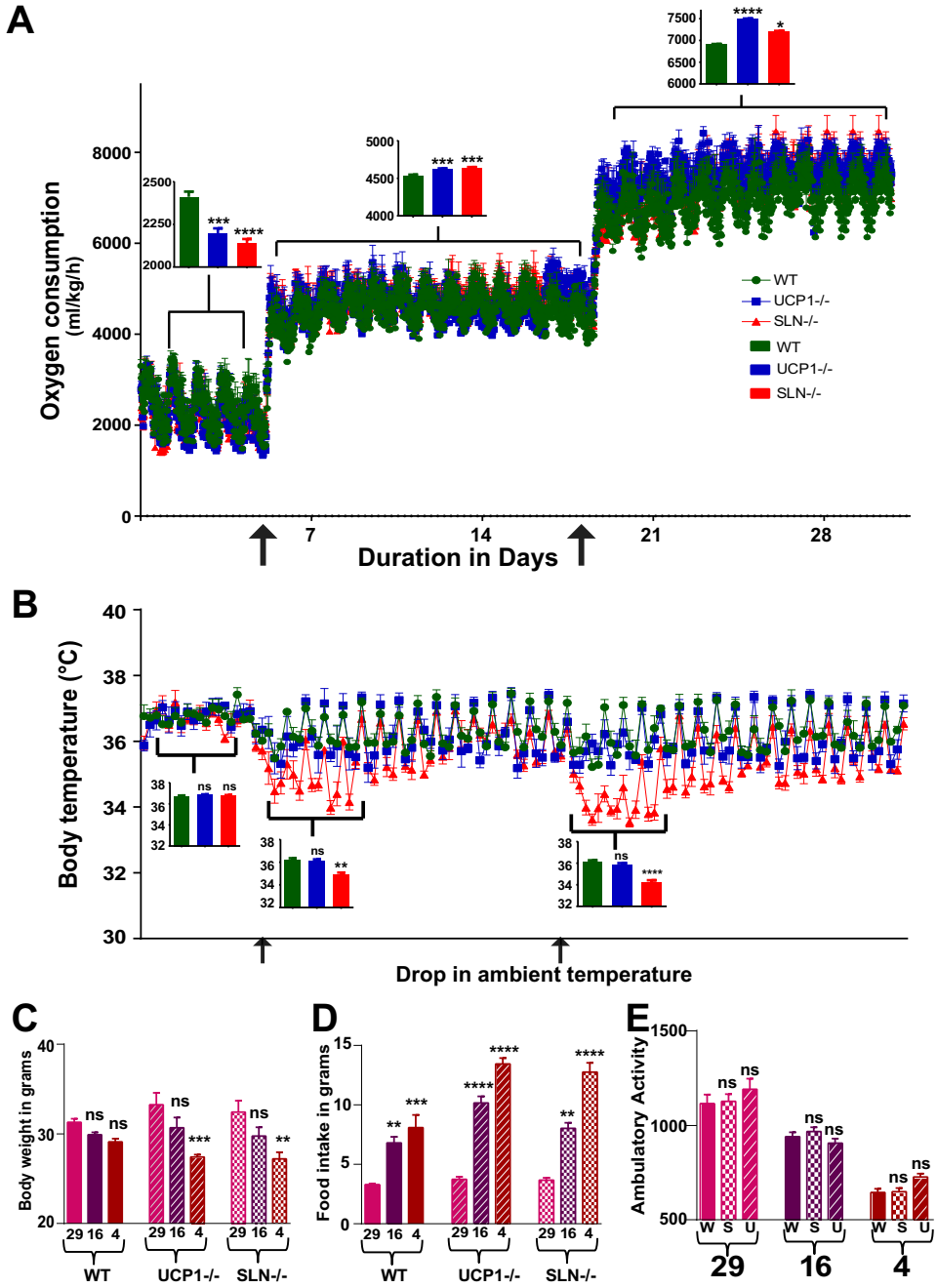

Figure 1. Physiological measurements of SLN$^{-/-}$ and UCP1$^{-/-}$ mice during cold adaptation. *A*, oxygen consumption during housing at 29.0 °C ± 1.0 °C, 16 °C ± 1.0 °C, and 4 °C ± 1.0 °C. The *insets* show average oxygen consumption for WT, UCP1$^{-/-}$, and SLN$^{-/-}$ at 29.0 °C ± 1.0 °C, 16 °C ± 1.0 °C, and 4 °C ± 1.0 °C. *B*, Tc as measured during the entire cold adaptation. Bar graphs show the average Tc during different cold exposure periods. *Black arrows* under the graphs indicate a switch in ambient temperature. *C*, body weight in grams at the end of the cold challenge. *D*, average food consumption per mouse per day in grams. *E*, ambulatory physical activity (*xy* axes) measured at different housing temperatures. Each break in the infrared beam is counted as one. One-way ANOVA test for multiple comparisons was performed to analyze statistical difference. The data for the WT at given ambient temperature were treated as a control for statistical analysis. Data from 6 animals/group were analyzed. *W*, wild type; *U*, UCP1$^{-/-}$; *S*, SLN$^{-/-}$. No statistical difference is labeled as *ns*.

mice showed a dramatic increase in SDH activity compared with SLN$^{-/-}$ muscle, suggesting that muscle-based (SLN-mediated) thermogenesis is activated to compensate for the loss of BAT activity. We also observed that loss of UCP1/BAT activity led to an up-regulation of SLN expression in red gastrocnemius and soleus muscle under mild and severe cold (Fig. 4, *B* and *C*). These data suggest increased reliance on muscle-based NST in UCP1$^{-/-}$ mice even under mild cold. Further, the skeletal muscle mitochondrial respiration capacity was significantly compromised in SLN$^{-/-}$ mice adapted to severe cold compared with their WT littermates (Fig. 4*D*). Electron microscopic analysis showed that mitochondrial abundance and ultrastructure underwent significant alteration in response to cold adaptation. Interestingly, quadriceps muscle of cold adapted UCP1$^{-/-}$ mice contained more intermyofibrillar mitochondria with elaborate crista structure compared with WT littermates (Fig. 5, *A*–*C*). The muscle tissues from UCP1$^{-/-}$ also contained a higher level of lipid droplets, indicating increased fatty acid oxi-

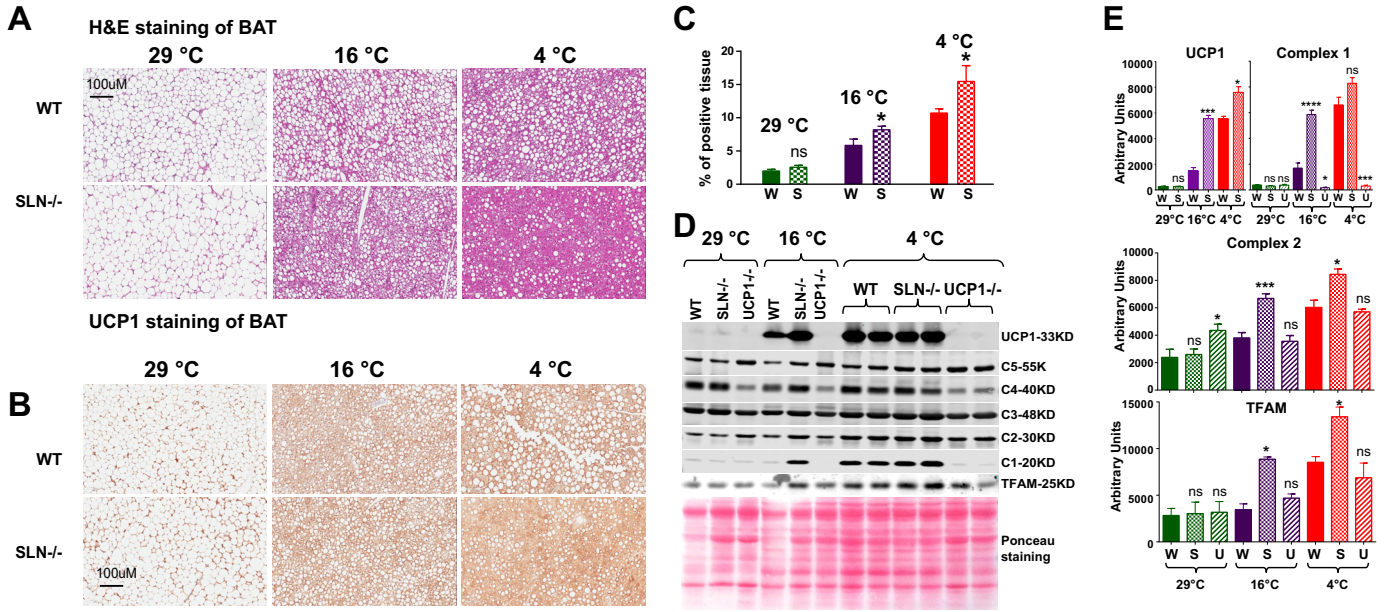

Figure 2. Cold-induced remodeling of BAT tissue in SLN$^{-/-}$ mice. *A*, H&E staining of BAT from SLN$^{-/-}$ and WT mouse littermates adapted to 29.0 °C ± 1.0 °C, 16 °C ± 1.0 °C, and 4 °C ± 1.0 °C. *B*, immunostaining of BAT with UCP1 antibody. *C*, quantification of UCP1 expression in BAT using the software Halo. The area with positive staining obtained for BAT from the UCP1$^{-/-}$ mice was taken as background and deducted from that obtained for WT and SLN$^{-/-}$ mice. *D*, representative Western blots of various mitochondrial proteins in BAT. Ponceau S staining is provided as a control to suggest equivalent loading. *C1*, complex I; *C2*, complex II; *C3*, complex III; *C4*, complex IV; *C5*, complex V, *i.e.* ATP synthase. The molecular masses of the detected bands are indicated. *E*, intensity of few of the proteins that show significant alteration after cold adaptation. Quantification of proteins was performed using ImageJ. *W*, wild type; *U*, UCP1$^{-/-}$; *S*, SLN$^{-/-}$. Statistical difference was analyzed using one-way ANOVA for multiple comparisons. No statistical difference is labeled as *ns*.

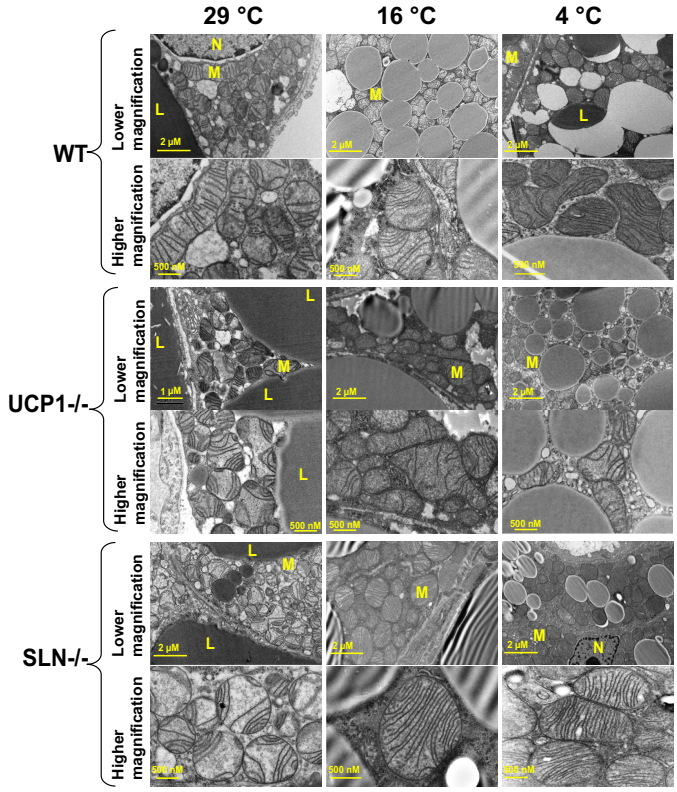

Figure 3. Electron microscopy of BAT from cold-adapted mice. Representative electron micrographs of BAT from cold-adapted mice are presented. The images presented as *top panels* and *bottom panels* for each genotype were obtained at low and high magnification, respectively. Housing temperature is indicated at the *top*. *N*, nucleus; *L*, lipid droplet; *M*, mitochondria. At thermoneutrality, mitochondria in BAT exhibit a very low abundance of crista structures irrespective of genotype. Interestingly, upon cold exposure, there is an increase in the abundance of mitochondrial cristae in WT and SLN$^{-/-}$ mice (*top* and *bottom rows*, respectively) but not in the UCP1$^{-/-}$ littermates.

dation and energy demand in muscle. However, cold-induced enhancement of intermyofibrillar mitochondrial abundance and ultrastructure was not observed in the muscle of SLN$^{-/-}$ mice. We further examined whether increased muscle thermogenesis requires enhanced vascularization to increase the supply of oxygen, humoral factors, and nutrients. CD31 staining shows that skeletal muscle from cold-adapted UCP1$^{-/-}$ mice has greater blood vessel density compared with WT littermates (Fig. 5, *D* and *E*). In contrast, blood vessel density did not significantly change in the muscle of cold-adapted SLN$^{-/-}$ mice. These data together suggest that SLN is essential for muscle-based thermogenesis.

Increased autonomic input to BAT in cold-exposed SLN$^{-/-}$ mice

Next, we wanted to investigate whether direct autonomic nervous input and adrenergic signaling to BAT is involved in the up-regulation of BAT function. We chose to investigate tyrosine hydroxylase (TH), a rate-limiting enzyme in the production of neurotransmitter epinephrine in the sympathetic neuron endings that innervate the BAT (20). The expression of TH was induced during cold adaptation in BAT (Fig. 6*A*). Interestingly, there is a greater induction of TH in the BAT of SLN$^{-/-}$ mice both under mild and extreme cold adaptation compared with the controls. Intriguingly, mild cold did not induce TH in UCP1$^{-/-}$ mice, whereas severe cold led to significant induction of TH. Neuropeptide Y (NPY) is another regulator of BAT function. NPY in the hypothalamus antagonizes epinephrine-mediated BAT activity (21–23). However, to our surprise, NPY levels were found to be higher in BAT of SLN$^{-/-}$ compared with WT mice in response to cold adaptation (Fig. 6, *B* and *C*). The immunohistochemistry data were further sup-

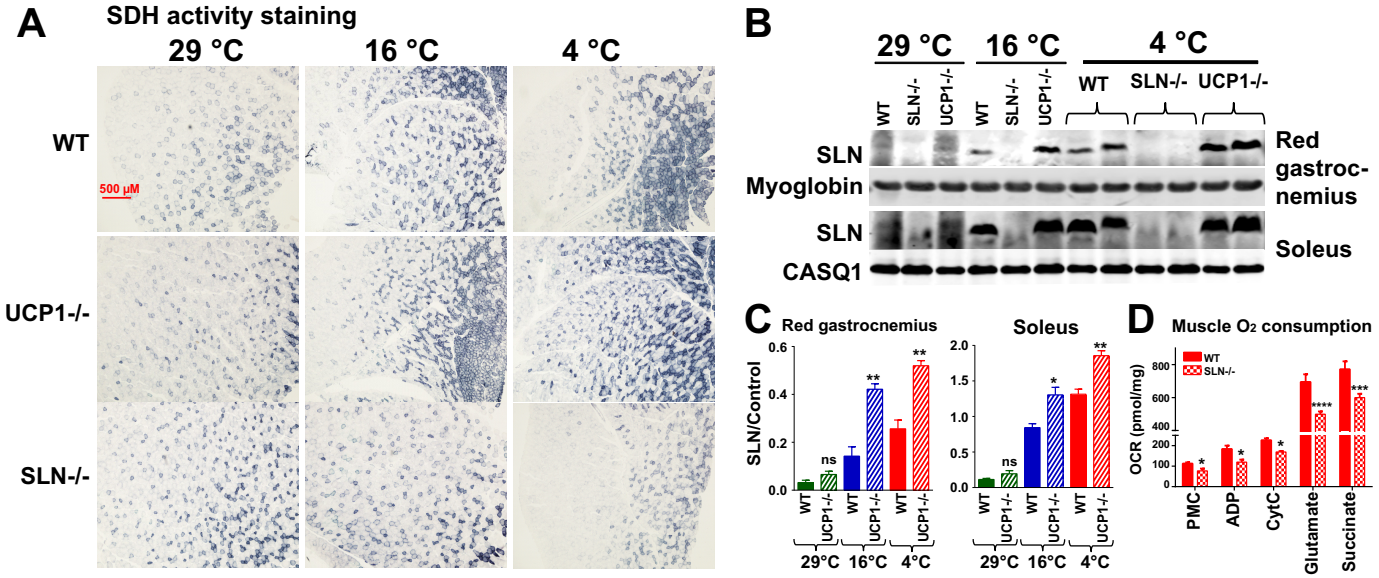

Figure 4. Up-regulation of oxidative metabolism and SLN in the skeletal muscle of UCP1$^{-/-}$ mice during cold adaptation. *A*, representative images showing SDH staining of skeletal muscle. *B*, Western blot of SLN showing increased expression after cold adaptation in UCP1$^{-/-}$ mice. Myoglobin and calsequestrin 1 (*CASQ1*) were used as internal loading controls. C, quantification of SLN expression in oxidative skeletal muscle after adaptation to cold. *D*, mitochondrial respiration of soleus muscle from WT and SLN$^{-/-}$ mice adapted to severe cold (4 °C). Statistical difference was analyzed using one-way ANOVA for multiple comparisons. No statistical difference is labeled as *ns*.

ported by Western blotting analysis of the NPY protein (Fig. 6*D*). We also investigated whether increased vascularization is an important determinant of enhanced BAT function. To detect neovascularization, we performed CD31 staining of BAT tissues from mild– and severe cold–adapted animals (Fig. 6*B*). The BAT from SLN$^{-/-}$ mice showed a significant increase in CD31 staining compared with the WT, suggesting increased reliance on BAT-based heat production (Fig. 6, *B* and *C*). UCP1$^{-/-}$ mice also showed an increase in CD31 staining, as reported previously (24). In addition to NPY, VEGF receptor 2 (VEGF-R2) plays an important role in the vascularization of BAT (25) and is vital for the performance and recruitment of NST in BAT. Western blotting analysis shows that SLN$^{-/-}$ adapted to mild cold expressed more VEGFR2 than WT littermates (Fig. 6, *D* and *E*). Adaptation to extreme cold led to significant up-regulation of VEGFR2 expression in the BAT from WT and SLN$^{-/-}$ mice. These observations are also supported by immunohistochemistry. Taken together, these data indicate that direct autonomic input and vascularization are important for increased recruitment of BAT under conditions where muscle-based NST is compromised.

Discussion

Homoeothermic mammals maintain a constant Tc through multiple thermogenic mechanisms (26). It is well-known that BAT and skeletal muscle are major sites of heat production (2, 27–29). Although BAT is known to generate heat through NST (UCP1-dependent uncoupling) (2, 30–33), some studies have questioned whether muscle has the ability to generate heat through NST (34). Other studies suggest a potential role for skeletal muscle in NST in human and animal models (18, 35–40). Nedergaard and co-workers argue (34, 41) that increased shivering is the only mechanism for cold adaptation in UCP1$^{-/-}$ mice and questioned the existence of muscle-based NST. We have reported earlier that SLN-mediated uncoupling of SERCA is an important contributor to NST in muscle (8–10, 12, 13, 42, 43). Therefore, in this study, we investigated whether SLN-based NST is up-regulated when BAT function is impaired and vice versa. This study took advantage of mild cold exposure (which does not evoke a shivering response) to investigate the recruitment of muscle- *versus* BAT-based NST mechanisms in UCP1$^{-/-}$ and SLN$^{-/-}$ mice. A key finding of this study was that exposure to mild cold was sufficient to cause significant up-regulation of UCP1 expression in SLN$^{-/-}$ mice, a level comparable with UCP1 expression seen in severe cold (4 °C). The increased recruitment of BAT is further supported by increased mitochondrial remodeling, as evident from ultrastructural studies and up-regulation of mitochondrial electron transport chain complex proteins. In addition, we have reported previously that adaptation of SLN$^{-/-}$ mice to 4 °C caused increased beiging of inguinal white adipose tissue (13). Taken together, this study provides experimental evidence that BAT-based thermogenesis is recruited to a greater extent in the absence of SLN, indicating that muscle is also an important site of NST and critical for cold adaptation.

In this study, we examined whether loss of UCP1 leads to increased reliance on muscle-based NST, especially under conditions of mild cold challenge, where shivering is not a major mechanism of thermogenesis (44). We found that mild cold exposure at 16 °C is sufficient to activate muscle-based thermogenesis, and this is evident even in WT control mice. Interestingly, mild cold adaptation led to a greater up-regulation of SLN expression in skeletal muscle of UCP1$^{-/-}$ mice compared with WT littermates. Our data also showed an increase in oxidative capacity in skeletal muscle of UCP1$^{-/-}$ mice compared with SLN$^{-/-}$ littermates. This was supported by an increased abun-

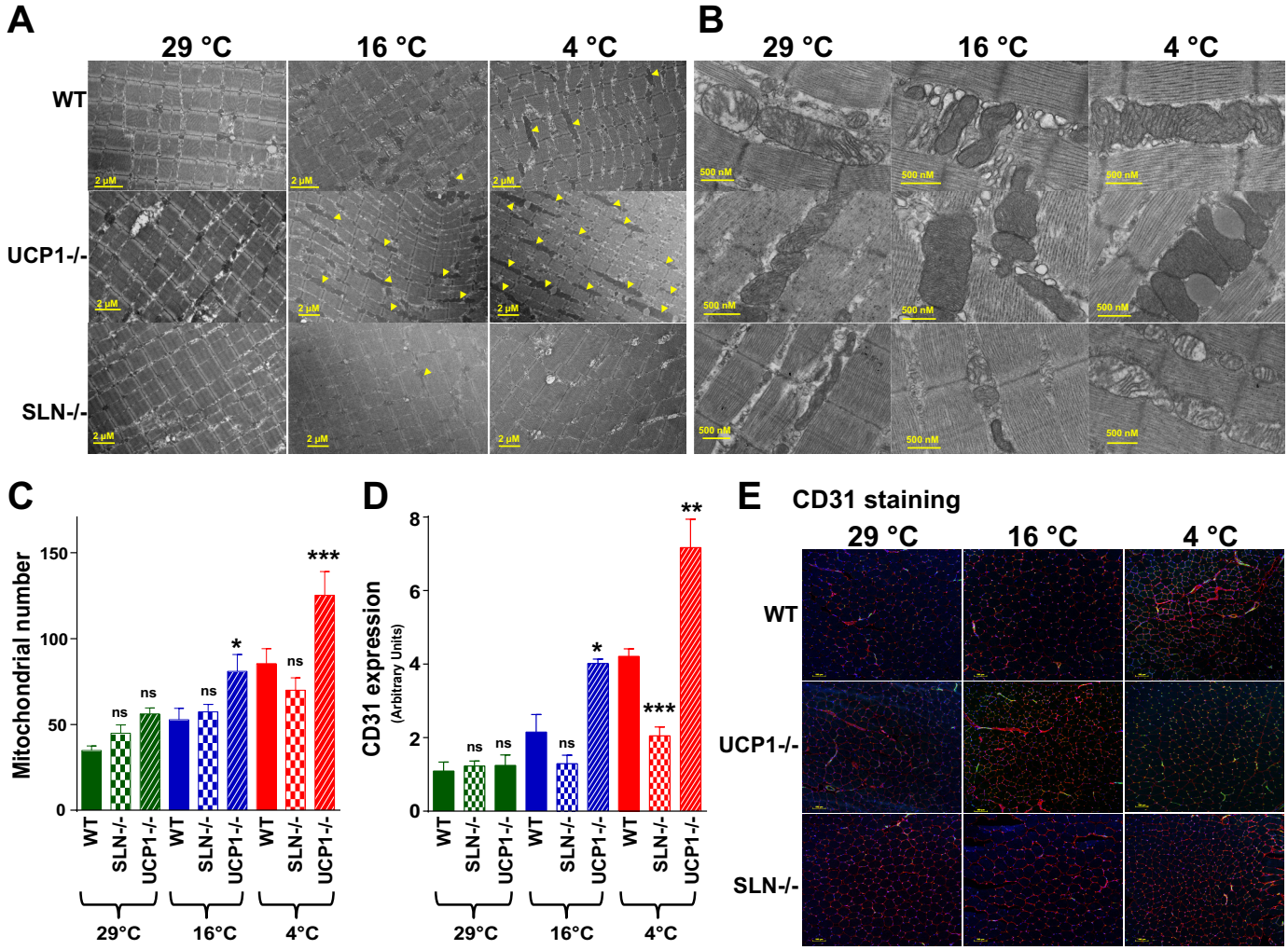

Figure 5. Increased recruitment of skeletal muscle thermogenesis in UCP1$^{-/-}$ mice. *A*, transmission electron micrographs of skeletal muscle showing intermyofibrillar mitochondrial abundance in quadriceps muscle. WT and UCP1$^{-/-}$ mice show higher mitochondrial abundance upon adaptation to cold. *B*, high-magnification electron micrographs showing intermyofibrillar mitochondria with an increased density of crista structures, especially in UCP1$^{-/-}$ mice acclimatized to cold. In contrast, intermyofibrillar mitochondria in muscles from SLN$^{-/-}$ mice do not show any elaboration of crista structures. *C*, number of mitochondria per low magnification electron micrographs. *D*, expression of anti-cluster of differentiation 31 (CD31) in skeletal muscle. *E*, representative image of immunostaining using anti-CD31 (*green*) and anti-laminin (*red*) antibodies to probe neovascularization of skeletal muscle. Statistical difference was analyzed using one-way ANOVA for multiple comparisons. No statistical difference is labeled as *ns*.

dance of intermyofibrillar mitochondria with elaborate crista structure in skeletal muscle of UCP1$^{-/-}$ mice compared with WT littermates. Increased neovascularization was more prominent in cold-adapted UCP1$^{-/-}$ mice, indicating augmented substrate/energy demand. Further, in UCP1$^{-/-}$ mice, the white fat amount decreased, whereas food consumption was higher, along with an increased abundance of lipid droplets in skeletal muscle, indicating enhanced muscle thermogenesis. Adaptation to severe cold (4 °C) also led to increased SLN expression in oxidative muscle in UCP1$^{-/-}$ mice. These findings, taken together, suggest that SLN-based thermogenesis can be recruited to compensate for loss of BAT activity.

We were intrigued how loss of SLN can lead to hyper-recruitment of BAT-based thermogenesis. Previous studies have shown that BAT-mediated thermogenesis is activated and regulated by direct innervation of autonomic neurons from the CNS and hypothalamus (45–47). The findings from this study show that loss of SLN led to an increase in expression of TH in BAT upon cold adaptation, indicating higher autonomic adrenergic input. This supports the initial observation that BAT is hyper-recruited in SLN$^{-/-}$ mice even under mild cold adaptation. We have reported earlier that systemic adrenergic hormone levels were not different between cold-adapted SLN$^{-/-}$ and WT littermates (13). These data suggest that hyper-recruitment of BAT in SLN$^{-/-}$ mice is not mediated by circulating adrenergic hormones but direct input from autonomic neurons. A novel finding of this study is that cold adaptation of SLN$^{-/-}$ mice caused a significant up-regulation of the neurotransmitter NPY in BAT; however, its role in BAT has not been fully defined. The observed increase in endogenous NPY could lead to increased vascularization of BAT, which is essential for the hyper-recruitment of BAT-based NST. This interpretation is also supported by increased expression of VEGF-R2 (known to promote neovascularization) and CD31 under mild cold adaptation in the BAT of SLN$^{-/-}$ mice. Based on these findings, we propose that NPY synergistically works with epinephrine to recruit BAT-based thermogenesis.

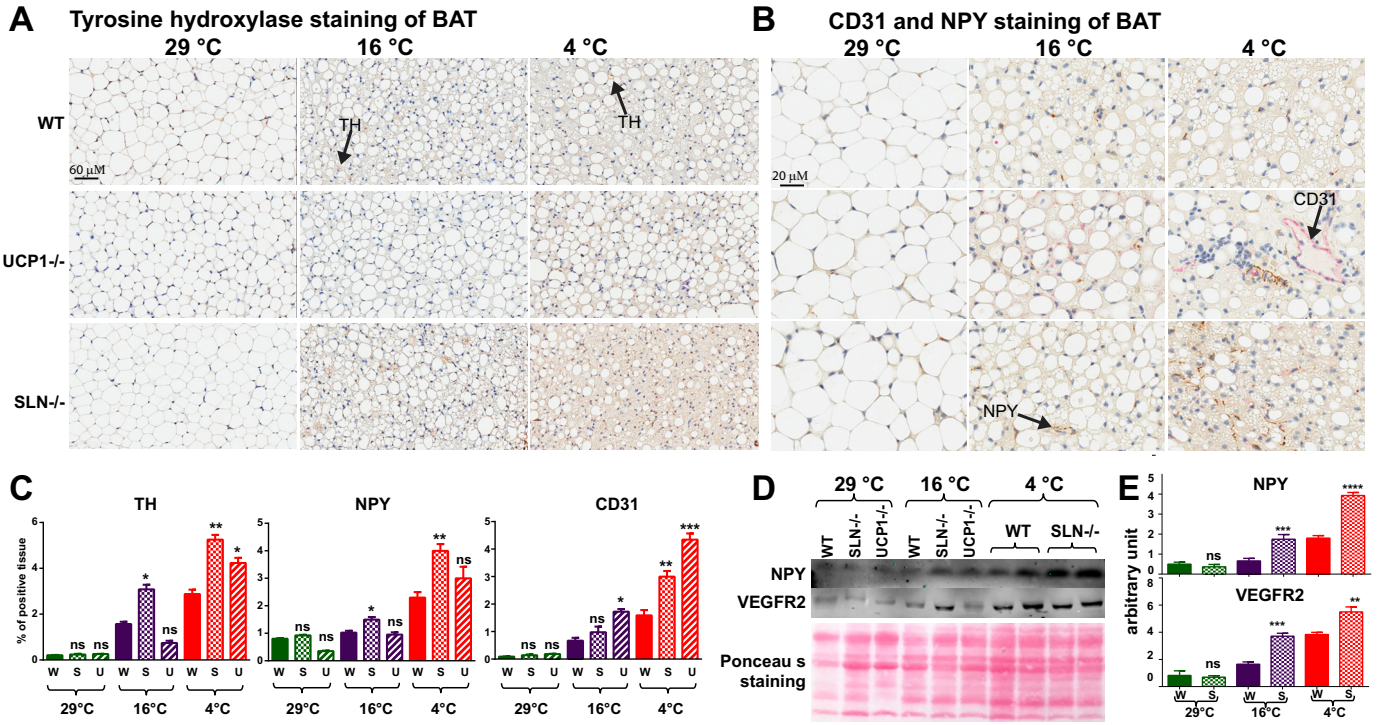

Figure 6. Increased recruitment of BAT-based thermogenesis in SLN$^{-/-}$ mice during cold adaptation. *A*, chromogenic staining (*brown*) of BAT with anti-TH antibody. The location of positive TH staining is shown by *black arrows*. *B*, representative images of BAT with anti-CD31 (*red*) and anti-NPY (*brown*) antibodies. Positive areas of staining are indicated by *black arrows*. *C*, quantification of positively stained areas for TH, NPY, and CD31. Quantification was performed using Halo software. W, wild type; *U*, UCP1$^{-/-}$; *S*, SLN$^{-/-}$. *D*, representative Western blotting of NPY and VEGF-R2. Ponceau S staining was provided as a control to indicate equivalent loading for all samples analyzed. *E*, quantification of NPY and VEGF-R2 protein expression in the BAT. Statistical difference was analyzed using one-way ANOVA for multiple comparisons. No statistical difference is labeled as *ns*.

BAT plays a crucial role in mammalian evolution and adaptation to cold from small rodents to large mammals (1, 48–51). In most mammals, including humans, BAT is highly abundant in neonatal stages and plays a dominant role during early postnatal development (52, 53), whereas skeletal muscles are still under development and not mature enough to be recruited for shivering (10). Hence, the presence of BAT in abundant quantities is beneficial for the survival of newborn babies; newborns often have to incur huge heat loss because of a greater surface-to-body ratio (48). In large mammals, the amount of BAT decreases in adult stages and remains localized to only a few sites in the body, and they mostly rely on skeletal muscle-based thermogenesis. Although recent studies have shown that BAT can be reactivated upon cold exposure in adult humans (54, 55), the relative contribution of activated BAT to thermogenesis awaits further clarification. The results from this study suggest that, although BAT is an efficient system to generate heat, even rodents rely on muscle-based NST for optimum temperature homeostasis. The two systems are complementary in their function, and when one system is impaired; the other comes to the rescue and maintains survival of the organism. The detailed mechanistic basis of how these two systems maintain a functional cross-talk is an emerging area of research (56–59). Several studies suggest that these organs communicate with each other through myokines and adipokines during high metabolic demand, including thermogenesis (14, 16, 60). Future research should examine how the autocrine and paracrine mechanisms contribute to maintaining temperature homeostasis.

Experimental procedures

The generation of UCP1$^{-/-}$ and SLN$^{-/-}$ mice has been described previously (9, 13, 33). Mice double heterozygous (UCP1$^{-/+}$; SLN$^{-/+}$) for UCP1 and SLN on a C57Bl/6J background reared at 29 °C ± 1 °C were intercrossed to obtain homozygous knockouts for individual proteins and WT controls. The study protocol was approved by the Ohio State University Institutional Animal Care and Use Committee. All animal procedures were carried out in our Association for Assessment and Accreditation of Laboratory Animal Care–accredited animal facility and conducted in accordance with the Guide for the Care and Use of Laboratory Animals. Male mice were maintained in a temperature-controlled room at 29 °C ± 1 °C and fed a chow diet (Harlan Labs, rodent diet 17% kcal/fat).

Cold adaptation

All cold exposures were carried out in a temperature-controlled metabolic chamber. SLN$^{-/-}$ (n = 11), UCP1$^{-/-}$ (n = 10), and WT (n = 13) mice previously maintained at 29 °C ± 1 °C were individually housed in the temperature-controlled unit. The ambient temperature was decreased to 16 °C and maintained for a period of 2 weeks, and four mice were removed from the experiment; tissues were harvested and snap-frozen in liquid nitrogen for future analysis. Then ambient temperature was decreased to 4 °C, and the remaining mice were housed at 4 °C for a further 2 weeks. Body temperature was monitored at the same time (9 a.m., 4 p.m., and 10 p.m.) every day using

implanted thermal transponders (IPTT300, Bio Medic Data System, Seaford, DE). Body weight and food consumption were measured twice weekly.

Metabolic monitoring

During the complete period of cold adaptation, oxygen consumption, carbon dioxide production, and physical activity were continuously measured by the Oxymax Comprehensive Lab Animal Monitoring System (CLAMS, Columbus Instruments, Columbus, OH). Heat was calculated using oxygen consumption and carbon dioxide production. Physical activity was analyzed by taking total of beam breaks for the *xy* axes only.

Measurement of mitochondrial respiration

Measurement of mitochondrial function (oxygen consumption) in permeabilized muscle fibers was performed at 37 °C using Oxygraph 2K (Oroboros Inc., Innsbruck, Austria) as described earlier (8).

Histology of BAT

BAT was fixed in 10% formalin and embedded in paraffin. These formalin-fixed, paraffin-embedded (FFPE) samples were sectioned at 5 μM on a Microm 350s microtome. The slides were air-dried overnight and stained with hematoxylin and eosin using the Thermo Shandon Sequenza system at room temperature. Images were collected using a compound microscope. Statistical analysis was performed applying one-way ANOVA using GraphPad Prism 6 software.

Electron microscopy and SDH activity staining of muscle tissues

Longitudinal sections of skeletal muscles were taken after the indicated period of cold adaptation and fixed with 1% glutaraldehyde solution. The samples were processed by the core facility. Electron micrographs were obtained using a Tecnai G2 Spirit transmission electron microscope (FEI, Hillsboro, OR). SDH activity staining was performed on sections of muscles as described earlier (43), and images were acquired using a compound microscope. Statistical analysis was performed applying one-way ANOVA using GraphPad Prism 6 software.

Immunohistochemistry of BAT

For UCP1 staining, 5 μM FFPE samples were stained using anti-UCP1 antibody (catalog no. ab10983, Abcam) at 1:1000 dilution for 2 h at room temperature after citrate antigen retrieval using a Biocare Decloaker pressure cooker. Secondary antibody from the Leica Bond Polymer Refine detection kit (DS9800) was used and enzymatically stained with ImmPACT DAB peroxidase (HRP) substrate (SK-4105). For NPY and CD31 dual staining, 5 μM FFPE samples were processed using the Leica Bond ChromoPlex 1 dual detection kit (DS9477) containing the DAB and alkaline phosphatase chromogens. Anti-NPY (catalog no. D7Y5A; dilution, 1:300) was obtained from Cell Signaling Technology, and anti-CD31 (catalog no. DIA-310; dilution, 1:25) was purchased from Dianova GmBH. The secondary antibody for the rabbit primary antibody was taken from the Leica Bond Polymer Refine detection kit (DS9800), and that for the rat primary was from Biocare Rat alkaline phosphatase-Polymer (RT518). For TH staining, the primary antibody (catalog no. ab76442; dilution, 1:2500) was obtained from Abcam. The rabbit secondary polymer and the DAB chromogen were from the Leica Bond Polymer Refine detection kit (DS9800). All slides were counterstained with hematoxylin. The slides were scanned using a Leica Aperio Scanscope XT using a ×20/0.75 Plan Apo Olympus objective. The percentage of positive expression was measured using the Halo^{TM} platform from Indica Labs, Inc. Tissues from at least two animals from each genotype and housing temperature were analyzed applying one-way ANOVA using GraphPad Prism 6.

Immunohistochemistry of muscle

The frozen samples were sectioned at 10 μM on a Leica 1900 cryostat. The slides were removed from a −80 °C freezer, allowed to come to room temperature, and stained using the Thermo Shandon Sequenza system. The muscle samples were dually stained for CD31 (DIA-310, clone SZ31, Dianova GmBH, used at a dilution of 1:25) and laminin (catalog no. PA1-16730, Thermo Fisher, used at a dilution of 1:1000). Immunofluorescence staining was achieved using the secondary antibodies Alexa Fluor 647 IgG (A21244, dilution of 1:250) and Alexa Fluor 488 IgG (A11006, dilution of 1:250) for laminin and CD31, respectively. The primary antibodies were treated for 2 h at room temperature and the secondary antibodies for 1 h at room temperature. At the final step, DAPI was applied for 5 min, and coverslips were applied using Prolong Gold Antifade Mountant (Thermo Fisher Scientific). The intensity of CD31 staining was measured using ImageJ software, and statistical difference was calculated applying one-way ANOVA using GraphPad Prism 6 software.

Western blotting

Protein levels were quantified using the Western blotting technique using our protocols published previously (8, 13). The primary antibodies used included oxidative phosphorylation antibody mixture (catalog no. MS604, used at 1:2000 dilution) from MitoSciences, anti-UCP1 (catalog no. MAB6158, used at 1:3000 dilution) from R&D Systems, anti-mitochondrial transcription factor A (Tfam, catalog no. sc-23588, used at 1:1000 dilution) from Santa Cruz Biotechnology Inc., anti-NPY (catalog no. D7Y5A, used at 1:500 dilution) from Cell Signaling Technology, anti-VEGF-R2 (catalog no. D5B1, used at 1:2000 dilution) from Cell Signaling Technology, anti-CASQ1 (catalog no. MA3-913, used at 1:2000 dilution) from Thermo Fisher Scientific, and anti-myoglobin antibody (catalog no. sc-74525, used at 1:3000 dilution) from Santa Cruz Biotechnology Inc. The anti-SLN (1:1000 dilution) antibody was custom-generated in the laboratory of M. P. Western blotting was repeated at least three times for each protein, and intensities were quantified using ImageJ. Statistical difference was analyzed using one-way ANOVA for multiple comparisons with GraphPad Prism 6 software. The data for the WT at each temperature were treated as a control for interpretation.

Author contributions—N. C. B. and M. P. conceived the study. N. C. B. and S. S. designed and conducted the animal studies. L. A. R. and S. K. M. maintained the animal colonies. S. K. M. performed the muscle oxygen consumption experiments. S. P. performed morphometric measurements and analysis. N. C. B., S. S., F. C. G. R., and S. K. M. were involved in the biochemical analysis of tissue samples. All authors analyzed the data and contributed to manuscript writing.

Acknowledgments—UCP1$^{-/-}$ mice were generously provided by Prof. Leslie Kozak. We thank Dr. Meghna Pant for critical reading of the manuscript. We also thank Drs. J. Nedergaard, M. Olfert, and S. Egginton for insightful discussions that helped us with interpretation of our data.

References

1. Oelkrug, R., Polymeropoulos, E. T., and Jastroch, M. (2015) Brown adipose tissue: physiological function and evolutionary significance. *J. Comp. Physiol. B* **185,** 587–606
2. Cannon, B., and Nedergaard, J. (2004) Brown adipose tissue: function and physiological significance. *Physiol. Rev.* **84,** 277–359
3. Azzu, V., and Brand, M. D. (2010) The on-off switches of the mitochondrial uncoupling proteins. *Trends Biochem. Sci.* **35,** 298–307
4. Nedergaard, J., Golozoubova, V., Matthias, A., Asadi, A., Jacobsson, A., and Cannon, B. (2001) UCP1: the only protein able to mediate adaptive non-shivering thermogenesis and metabolic inefficiency. *Biochim. Biophys. Acta* **1504,** 82–106
5. Fedorenko, A., Lishko, P. V., and Kirichok, Y. (2012) Mechanism of fatty-acid-dependent UCP1 uncoupling in brown fat mitochondria. *Cell* **151,** 400–413
6. Davis, T. R. (1967) Contribution of skeletal muscle to nonshivering thermogenesis in the dog. *Am. J. Physiol.* **213,** 1423–1426
7. Greenway, D. C., and Himms-Hagen, J. (1978) Increased calcium uptake by muscle mitochondria of cold-acclimated rats. *Am. J. Physiol.* **234,** C7–C13
8. Bal, N. C., Maurya, S. K., Singh, S., Wehrens, X. H., and Periasamy, M. (2016) Increased reliance on muscle-based thermogenesis upon acute minimization of brown adipose tissue function. *J. Biol. Chem.* **291,** 17247–17257
9. Bal, N. C., Maurya, S. K., Sopariwala, D. H., Sahoo, S. K., Gupta, S. C., Shaikh, S. A., Pant, M., Rowland, L. A., Bombardier, E., Goonasekera, S. A., Tupling, A. R., Molkentin, J. D., and Periasamy, M. (2012) Sarcolipin is a newly identified regulator of muscle-based thermogenesis in mammals. *Nat. Med.* **18,** 1575–1579
10. Pant, M., Bal, N. C., and Periasamy, M. (2015) Cold adaptation overrides developmental regulation of sarcolipin expression in mice skeletal muscle: SOS for muscle-based thermogenesis? *J. Exp. Biol.* **218,** 2321–2325
11. Sahoo, S. K., Shaikh, S. A., Sopariwala, D. H., Bal, N. C., Bruhn, D. S., Kopec, W., Khandelia, H., and Periasamy, M. (2015) The N terminus of sarcolipin plays an important role in uncoupling sarco-endoplasmic reticulum Ca^{2+}-ATPase (SERCA) ATP hydrolysis from Ca^{2+} transport. *J. Biol. Chem.* **290,** 14057–14067
12. Sahoo, S. K., Shaikh, S. A., Sopariwala, D. H., Bal, N. C., and Periasamy, M. (2013) Sarcolipin protein interaction with sarco(endo)plasmic reticulum Ca^{2+} ATPase (SERCA) is distinct from phospholamban protein, and only sarcolipin can promote uncoupling of the SERCA pump. *J. Biol. Chem.* **288,** 6881–6889
13. Rowland, L. A., Bal, N. C., Kozak, L. P., and Periasamy, M. (2015) Uncoupling protein 1 and sarcolipin are required to maintain optimal thermogenesis, and loss of both systems compromises survival of mice under cold stress. *J. Biol. Chem.* **290,** 12282–12289
14. Rodríguez, A., Becerril, S., Ezquerro, S., Méndez-Giménez, L., and Frühbeck, G. (2017) Cross-talk between adipokines and myokines in fat browning. *Acta Physiol.* (*Oxf.*) **219,** 362–381, 10.1111/apha.12686
15. Dong, J., Dong, Y., Dong, Y., Chen, F., Mitch, W. E., and Zhang, L. (2016) Inhibition of myostatin in mice improves insulin sensitivity via irisin-mediated cross talk between muscle and adipose tissues. *Int. J. Obes.* **40,** 434–442
16. Trayhurn, P., Drevon, C. A., and Eckel, J. (2011) Secreted proteins from adipose tissue and skeletal muscle: adipokines, myokines and adipose/muscle cross-talk. *Arch. Physiol. Biochem.* **117,** 47–56
17. Giorgino, F. (2009) Adipose tissue function and dysfunction: organ cross talk and metabolic risk. *Am. J. Physiol. Endocrinol. Metab.* **297,** E975–E976
18. Wakabayashi, H., Nishimura, T., Wijayanto, T., Watanuki, S., and Tochihara, Y. (2017) Effect of repeated forearm muscle cooling on the adaptation of skeletal muscle metabolism in humans. *Int. J. Biometeorol.* **61,** 1261–1267
19. Feldmann, H. M., Golozoubova, V., Cannon, B., and Nedergaard, J. (2009) UCP1 ablation induces obesity and abolishes diet-induced thermogenesis in mice exempt from thermal stress by living at thermoneutrality. *Cell Metab.* **9,** 203–209
20. De Matteis, R., Ricquier, D., and Cinti, S. (1998) TH-, NPY-, SP-, and CGRP-immunoreactive nerves in interscapular brown adipose tissue of adult rats acclimated at different temperatures: an immunohistochemical study. *J. Neurocytol.* **27,** 877–886
21. Chen, P., Williams, S. M., Grove, K. L., and Smith, M. S. (2004) Melanocortin 4 receptor-mediated hyperphagia and activation of neuropeptide Y expression in the dorsomedial hypothalamus during lactation. *J. Neurosci.* **24,** 5091–5100
22. McCarthy, H. D., Kilpatrick, A. P., Trayhurn, P., and Williams, G. (1993) Widespread increases in regional hypothalamic neuropeptide Y levels in acute cold-exposed rats. *Neuroscience* **54,** 127–132
23. Shi, Y. C., Lau, J., Lin, Z., Zhang, H., Zhai, L., Sperk, G., Heilbronn, R., Mietzsch, M., Weger, S., Huang, X. F., Enriquez, R. F., Baldock, P. A., Zhang, L., Sainsbury, A., Herzog, H., and Lin, S. (2013) Arcuate NPY controls sympathetic output and BAT function via a relay of tyrosine hydroxylase neurons in the PVN. *Cell Metab.* **17,** 236–248
24. Xue, Y., Petrovic, N., Cao, R., Larsson, O., Lim, S., Chen, S., Feldmann, H. M., Liang, Z., Zhu, Z., Nedergaard, J., Cannon, B., and Cao, Y. (2009) Hypoxia-independent angiogenesis in adipose tissues during cold acclimation. *Cell Metab.* **9,** 99–109
25. Fredriksson, J. M., Nikami, H., and Nedergaard, J. (2005) Cold-induced expression of the VEGF gene in brown adipose tissue is independent of thermogenic oxygen consumption. *FEBS Lett.* **579,** 5680–5684
26. Silva, J. E. (2011) Physiological importance and control of non-shivering facultative thermogenesis. *Front. Biosci.* **3,** 352–371
27. Pant, M., Bal, N. C., and Periasamy, M. (2016) Sarcolipin: a key thermogenic and metabolic regulator in skeletal muscle. *Trends Endocrinol. Metab.* **27,** 881–892
28. Gamu, D., Bombardier, E., Smith, I. C., Fajardo, V. A., and Tupling, A. R. (2014) Sarcolipin provides a novel muscle-based mechanism for adaptive thermogenesis. *Exerc. Sport Sci. Rev.* **42,** 136–142
29. Block, B. A. (1994) Thermogenesis in muscle. *Annu. Rev. Physiol.* **56,** 535–577
30. Klingenspor, M., Fromme, T., Hughes, D. A., Jr., Manzke, L., Polymeropoulos, E., Riemann, T., Trzcionka, M., Hirschberg, V., and Jastroch, M. (2008) An ancient look at UCP1. *Biochim. Biophys. Acta* **1777,** 637–641
31. Ricquier, D. (2017) UCP1, the mitochondrial uncoupling protein of brown adipocyte: a personal contribution and a historical perspective. *Biochimie* **134,** 3–8
32. Klingenspor, M. (2003) Cold-induced recruitment of brown adipose tissue thermogenesis. *Exp. Physiol.* **88,** 141–148
33. Enerback, S., Jacobsson, A., Simpson, E. M., Guerra, C., Yamashita, H., Harper, M. E., and Kozak, L. P. (1997) Mice lacking mitochondrial uncoupling protein are cold-sensitive but not obese. *Nature* **387,** 90–94
34. Aydin, J., Shabalina, I. G., Place, N., Reiken, S., Zhang, S. J., Bellinger, A. M., Nedergaard, J., Cannon, B., Marks, A. R., Bruton, J. D., and Westerblad, H. (2008) Nonshivering thermogenesis protects against defective calcium handling in muscle. *FASEB J.* **22,** 3919–3924
35. Blondin, D. P., Daoud, A., Taylor, T., Tingelstad, H. C., Bézaire, V., Richard, D., Carpentier, A. C., Taylor, A. W., Harper, M. E., Aguer, C., and Haman, F. (2017) Four-week cold acclimation in adult humans shifts uncoupling thermogenesis from skeletal muscles to BAT. *J. Physiol.* **595,** 2099–2113

36. McKay, W. P., Vargo, M., Chilibeck, P. D., and Daku, B. L. (2013) Effects of ambient temperature on mechanomyography of resting quadriceps muscle. *Appl. Physiol. Nutr. Metab.* **38,** 227–233
37. Loiselle, D. S., Johnston, C. M., Han, J. C., Nielsen, P. M., and Taberner, A. J. (2016) Muscle heat: a window into the thermodynamics of a molecular machine. *Am. J. Physiol. Heart Circ. Physiol.* **310,** H311–H325
38. Reis, M., Farage, M., and de Meis, L. (2002) Thermogenesis and energy expenditure: control of heat production by the Ca^{2+}-ATPase of fast and slow muscle. *Mol. Membr. Biol.* **19,** 301–310
39. Anunciado-Koza, R. P., Zhang, J., Ukropec, J., Bajpeyi, S., Koza, R. A., Rogers, R. C., Cefalu, W. T., Mynatt, R. L., and Kozak, L. P. (2011) Inactivation of the mitochondrial carrier SLC25A25 (ATP-Mg^{2+}/Pi transporter) reduces physical endurance and metabolic efficiency in mice. *J. Biol. Chem.* **286,** 11659–11671
40. Kanatous, S. B., Hawke, T. J., Trumble, S. J., Pearson, L. E., Watson, R. R., Garry, D. J., Williams, T. M., and Davis, R. W. (2008) The ontogeny of aerobic and diving capacity in the skeletal muscles of Weddell seals. *J. Exp. Biol.* **211,** 2559–2565
41. Golozoubova, V., Hohtola, E., Matthias, A., Jacobsson, A., Cannon, B., and Nedergaard, J. (2001) Only UCP1 can mediate adaptive nonshivering thermogenesis in the cold. *FASEB J.* **15,** 2048–2050
42. Bombardier, E., Smith, I. C., Gamu, D., Fajardo, V. A., Vigna, C., Sayer, R. A., Gupta, S. C., Bal, N. C., Periasamy, M., and Tupling, A. R. (2013) Sarcolipin trumps β-adrenergic receptor signaling as the favored mechanism for muscle-based diet-induced thermogenesis. *FASEB J.* **27,** 3871–3878
43. Maurya, S. K., Bal, N. C., Sopariwala, D. H., Pant, M., Rowland, L. A., Shaikh, S. A., and Periasamy, M. (2015) Sarcolipin is a key determinant of the basal metabolic rate, and its overexpression enhances energy expenditure and resistance against diet-induced obesity. *J. Biol. Chem.* **290,** 10840–10849
44. Nishimura, T., Motoi, M., Egashira, Y., Choi, D., Aoyagi, K., and Watanuki, S. (2015) Seasonal variation of non-shivering thermogenesis (NST) during mild cold exposure. *J. Physiol. Anthropol.* **34,** 11
45. Zaretskaia, M. V., Zaretsky, D. V., Shekhar, A., and DiMicco, J. A. (2002) Chemical stimulation of the dorsomedial hypothalamus evokes non-shivering thermogenesis in anesthetized rats. *Brain Res.* **928,** 113–125
46. Labbé, S. M., Caron, A., Lanfray, D., Monge-Rofarello, B., Bartness, T. J., and Richard, D. (2015) Hypothalamic control of brown adipose tissue thermogenesis. *Front. Syst. Neurosci.* **9,** 150
47. Tupone, D., Madden, C. J., and Morrison, S. F. (2014) Autonomic regulation of brown adipose tissue thermogenesis in health and disease: potential clinical applications for altering BAT thermogenesis. *Front. Neurosci.* **8,** 14
48. Rowland, L. A., Bal, N. C., and Periasamy, M. (2015) The role of skeletal-muscle-based thermogenic mechanisms in vertebrate endothermy. *Biol. Rev. Camb. Philos. Soc.* **90,** 1279–1297
49. Oelkrug, R., Goetze, N., Exner, C., Lee, Y., Ganjam, G. K., Kutschke, M., Müller, S., Stöhr, S., Tschöp, M. H., Crichton, P. G., Heldmaier, G., Jastroch, M., and Meyer, C. W. (2013) Brown fat in a protoendothermic mammal fuels eutherian evolution. *Nat. Commun.* **4,** 2140
50. Saito, S., Saito, C. T., and Shingai, R. (2008) Adaptive evolution of the uncoupling protein 1 gene contributed to the acquisition of novel nonshivering thermogenesis in ancestral eutherian mammals. *Gene* **408,** 37–44
51. Jastroch, M., Wuertz, S., Kloas, W., and Klingenspor, M. (2005) Uncoupling protein 1 in fish uncovers an ancient evolutionary history of mammalian nonshivering thermogenesis. *Physiol. Genomics* **22,** 150–156
52. Dawkins, M. J., and Scopes, J. W. (1965) Non-shivering thermogenesis and brown adipose tissue in the human new-born infant. *Nature* **206,** 201–202
53. Lean, M. E., James, W. P., Jennings, G., and Trayhurn, P. (1986) Brown adipose tissue uncoupling protein content in human infants, children and adults. *Clin. Sci.* **71,** 291–297
54. Nedergaard, J., Bengtsson, T., and Cannon, B. (2007) Unexpected evidence for active brown adipose tissue in adult humans. *Am. J. Physiol. Endocrinol. Metab.* **293,** E444–E452
55. van Marken Lichtenbelt, W. D., Vanhommerig, J. W., Smulders, N. M., Drossaerts, J. M., Kemerink, G. J., Bouvy, N. D., Schrauwen, P., and Teule, G. J. (2009) Cold-activated brown adipose tissue in healthy men. *N. Engl. J. Med.* **360,** 1500–1508
56. Pedersen, B. K., and Febbraio, M. A. (2012) Muscles, exercise and obesity: skeletal muscle as a secretory organ. *Nature reviews. Endocrinology* **8,** 457–465
57. Rodríguez, A., Becerril, S., Ezquerro, S., Méndez-Giménez, L., and Frühbeck, G. (2017) Crosstalk between adipokines and myokines in fat browning. *Acta Physiologica* **219,** 362–381
58. Indrakusuma, I., Sell, H., and Eckel, J. (2015) Novel mediators of adipose tissue and muscle crosstalk. *Curr. Obes. Rep.* **4,** 411–417
59. Huang-Doran, I., Zhang, C. Y., and Vidal-Puig, A. (2017) Extracellular vesicles: novel mediators of cell communication in metabolic disease. *Trends Endocrinol. Metab.* **28,** 3–18
60. Li, F., Li, Y., Duan, Y., Hu, C. A., Tang, Y., and Yin, Y. (2017) Myokines and adipokines: involvement in the crosstalk between skeletal muscle and adipose tissue. *Cytokine Growth Factor Rev.* **33,** 73–82